ADVANCED FUNCTIONAL MATERIALS
www.afm-journal.de

Biodegradable, Sustainable Hydrogel Actuators with Shape and Stiffness Morphing Capabilities via Embedded 3D Printing

*Wenhuan Sun, Avery S. Williamson, Ravesh Sukhnandan, Carmel Majidi, Lining Yao, Adam W. Feinberg, and Victoria A. Webster-Wood**

Despite the impressive performance of recent marine robots, many of their components are non-biodegradable or even toxic and may negatively impact sensitive ecosystems. To overcome these limitations, biologically-sourced hydrogels are a candidate material for marine robotics. Recent advances in embedded 3D printing have expanded the design freedom of hydrogel additive manufacturing. However, 3D printing small-scale hydrogel-based actuators remains challenging. In this study, Free form reversible embedding of suspended hydrogels (FRESH) printing is applied to fabricate small-scale biologically-derived, marine-sourced hydraulic actuators by printing thin-wall structures that are water-tight and pressurizable. Calcium-alginate hydrogels are used, a sustainable biomaterial sourced from brown seaweed. This process allows actuators to have complex shapes and internal cavities that are difficult to achieve with traditional fabrication techniques. Furthermore, it demonstrates that fabricated components are biodegradable, safely edible, and digestible by marine organisms. Finally, a reversible chelation-crosslinking mechanism is implemented to dynamically modify alginate actuators' structural stiffness and morphology. This study expands the possible design space for biodegradable marine robots by improving the manufacturability of complex soft devices using biologically-sourced materials.

1. Introduction

Robots are becoming increasingly ubiquitous beyond the lab. As technology advances, robots are increasingly common in manufacturing, homes for cleaning, delivery services, search and rescue, and exploring challenging environments worldwide, including fragile marine ecosystems. With growing adoption in marine sciences, it is essential to consider the safety and environmental impact of deploying aquatic robots. They may interact with living organisms, become lost, or break while deployed. Unfortunately, many existing robotic technologies rely on rigid actuators composed of metals and plastics, which may harm aquatic organisms directly through contact and ingestion or indirectly by accumulating non-biodegradable materials in the environment.

Soft, compliant actuation allows robots to interact safely with living organisms.[1] Recent material science and manufacturing

W. Sun, A. S. Williamson, R. Sukhnandan, C. Majidi, V. A. Webster-Wood
Department of Mechanical Engineering
Carnegie Mellon University
5000 Forbes Ave, Pittsburgh, PA 15213, USA
E-mail: vwebster@andrew.cmu.edu

C. Majidi, A. W. Feinberg, V. A. Webster-Wood
Department of Biomedical Engineering
Carnegie Mellon University
5000 Forbes Ave, Pittsburgh, PA 15213, USA

C. Majidi, V. A. Webster-Wood
Robotics Institute
Carnegie Mellon University
5000 Forbes Ave, Pittsburgh, PA 15213, USA

The ORCID identification number(s) for the author(s) of this article can be found under https://doi.org/10.1002/adfm.202303659

DOI: 10.1002/adfm.202303659

C. Majidi, A. W. Feinberg
Department of Materials Science and Engineering
Carnegie Mellon University
5000 Forbes Ave, Pittsburgh, PA 15213, USA

C. Majidi
Department of Electrical and Computer Engineering
Carnegie Mellon University
5000 Forbes Ave, Pittsburgh, PA 15213, USA

C. Majidi
Department of Civil & Environmental Engineering
Carnegie Mellon University
5000 Forbes Ave, Pittsburgh, PA 15213, United States

L. Yao
Human-Computer Interaction Institute, School of Computer Science
Carnegie Mellon University
5000 Forbes Ave, Pittsburgh, PA 15213, USA

A. W. Feinberg, V. A. Webster-Wood
McGowan Institute for Regenerative Medicine
Carnegie Mellon University
5000 Forbes Ave, Pittsburgh, PA 15213, USA

advances have enabled significant progress in soft actuation using unconventional building materials.[2] For example, biomimetic soft robots based on shape memory alloy (SMA) have achieved biologically relevant speeds.[3] Additionally, several SMA,[4] shape memory polymer (SMP),[5,6] and fluidic elastomer[7,8] based grippers have been reported to be capable of handling objects more than 20 times their weight.[9] However, many soft robot materials, such as polydimethylsiloxane, polystyrene, polytetrafluoroethylene, acrylonitrile butadiene styrene, and silver epoxy, are not biodegradable or are even toxic, which can pose potential hazards to the environment if deployed in marine ecosystems.

In considering the environmental impact of deployed robots, several strategies have been explored for biodegradable and sustainable soft actuators.[9,10] Some promising candidate materials include hydrogels, which are polymer networks that may be biodegradable[11] and stimuli-responsive.[5] In addition to extensive applications in tissue engineering,[12] drug delivery,[13] and wound dressing,[14] hydrogels have been used to fabricate soft actuators[15] with osmotic,[16] cell-powered,[17] magnetic,[11] acoustic,[18] hydraulic/pneumatic,[19] and electrohydraulic actuation.[20]

However, fabricating soft hydrogel structures can be challenging. Compared with traditional methods, such as mold casting, 3D printing greatly increases geometric design freedom. Unfortunately, many hydrogels are too soft to support their weight during printing. To overcome this challenge, embedded printing can be used, where hydrogels are extruded into a fugitive support bath.[21–28] A state-of-the-art embedded printing technique is Freeform Reversible Embedding of Suspended Hydrogels (FRESH),[22,23] in which hydrogels are crosslinked in a bath of gelatin microparticles that provide support during printing and liquefy with elevated temperature for part retrieval. FRESH has enabled the printing of complex hydrogel structures, including human heart phantoms at full organ scale.[22,29] Such approaches show great potential for creating soft, biodegradable robots.

Toward addressing the need for biodegradable actuators for deployment in marine ecosystems, in this study, we present the application of FRESH printing to fabricating biologically-derived marine-sourced hydrogel actuators using calcium-alginate (**Figure 1**). For FRESH-printed actuators (Figure 1A,B) to be applicable and advantageous in soft marine robots, they must: (1) be water-tight, (2) exhibit repeatable and reliable motion and force (Figure 1C), and (3) enable additional design freedom over traditional fabrication approaches. In this paper, we show that tailoring the ionic crosslinking process and print pathing are critical to achieving water-tight FRESH-printed alginate actuators that meet each of these needs, demonstrating their utility in soft grasping (Figure 1D). Furthermore, we use this approach to create novel soft actuators that are (1) biodegradable (Figure 1F), (2) edible by marine organisms (Figure 1E), and (3) exhibit shape and stiffness morphing capabilities. These capabilities will allow researchers to design and manufacture soft robots that can be safely deployed in aquatic environments, interact with delicate plants and animals, and safely degrade following mission completion.

2. Results

2.1. Water-Tight FRESH-Printed Actuators Exhibit Reliable Bending and Linear Motions

To demonstrate the application of the FRESH technique for functional soft actuator fabrication, we first manufactured a Pneu-Net[37] style bending actuator (Figures 1A–C and 2A,B). To achieve watertightness, modifications were made to the standard operating procedures previously reported for FRESH printing of alginate to control the rate and extent of ionic crosslinking.[23,38] In particular, we found that the standard calcium chloride ($CaCl_2$) concentration in the gelatin support slurry was too high, resulting in actuators that did not maintain water-tightness. Watertightness of the actuators is directly related to filament fusion and crosslinking between layers during printing. If the $CaCl_2$ concentration in the slurry is too high, filament crosslinking occurs too rapidly before layers fully fuse; if the $CaCl_2$ concentration is too low, then crosslink density is too low, resulting in actuators that are too soft and fragile to handle. To achieve water-tightness, $CaCl_2$ concentration in the support bath material was reduced from 0.1% (w/v)[23] to 0.05% (w/v), which slowed crosslinking of extruded alginate filaments to facilitate fusion between adjacent filaments. Due to the reduced $CaCl_2$ concentration, actuators were incubated in the slurry for 20–60 min, depending on print size, to increase ionic crosslink density after printing and before further processing. To further strengthen actuators, a high-concentration (2.5% (w/v)) $CaCl_2$ solution was used for slurry liquefaction and subsequent storage to maximize ionic crosslink density for improved actuator durability and robustness. These modifications to the FRESH standard protocol allowed water-tight actuators to be reliably printed.

We tested bending actuator's performance under cyclic loading conditions with a range of input flow rates while tracking actuator motion (Figure 2C,D). The FRESH-printed bending actuators can operate at a range of frequencies and are robust during extended operation. The actuator showed a swift response (maximum actuation frequency: 1.25 Hz) to the eight different input flow rates explored in this study (1, 2, 4, 5, 6, 7, 8 mL min^{-1}) and the rise time (time the actuator takes to move from its minimum and maximum bending positions, Figure 2A) decreased with higher flow rates (Figure 2B). When operated at the maximum frequency tested (1.25 Hz, flow rate: 8 mL min^{-1}) for 500 cycles, the actuators showed a consistent angular deflection motion profile (10.13 ± 0.31°, mean ± standard deviation) with only a 2.68% decrease in amplitude across the 500 cycles tested (Figure 2C). Similarly, the measured pressure changes within each actuation cycle also showed a consistent profile (2.51 ± 0.19 kPa) with a 6.69% drop in pressure range (Figure 2D). During high cycle unloaded testing, the bending actuator deflection angle decreased more than 60% over the first 5 hr period of continuous cyclic actuation (Figure S5, Supporting Information). This represents a 3.4×10^{-3}% decrease in bending angle per actuation cycle over this 5-h window. These results demonstrate the robustness of these FRESH-printed bending actuators for short-term operation on the order of hours.

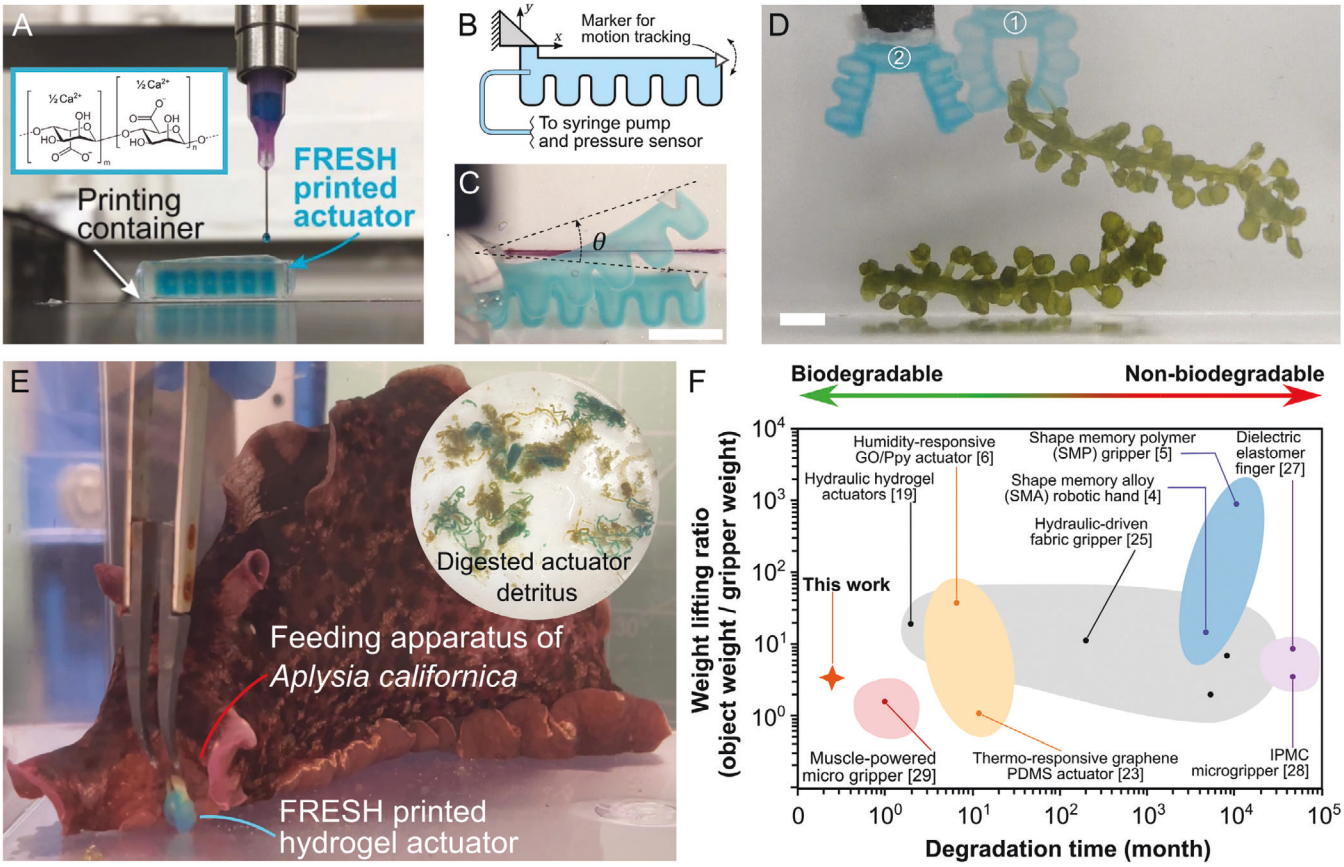

Figure 1. A) Biodegradable, edible, morphing hydraulic actuators are fabricated using a biologically-sourced ink using FRESH printing. B,C) Individual actuators have been characterized using motion tracking, force, and pressure measurements. Scale bar: 5 mm. D) This approach can be used to fabricate small-scale soft robotic systems capable of delicate object handling, such as manipulating the sea grape shown here using an alginate-based FRESH-printed robot gripper. Scale bar: 5 mm. E) Our biologically-sourced hydraulic actuators are biodegradable and safely edible by marine organisms and can be safely digested (see inset). F) Comparison of the weight lifting ratio and degradation time between FRESH-printed grippers in this study and representative soft robotic grippers, grouped and color-coded based on actuation mechanisms (stimuli-responsive polymers,[6,30] hydraulic actuation,[19,31–33] shape memory alloys and polymers,[4,5] electro-responsive polymers,[34,35] and cell-powered actuation[36]). Weight lifting ratios are displayed as reported in the original publications, and the degradation time is estimated based on the building materials of soft grippers.

In addition to hydraulic-driven bending actuators, we used FRESH to fabricate a linear actuator (Figure 2E) and analyzed its motion profile using motion tracking (Figure 2F) and blocking force under cyclic loading conditions. The linear actuator shows consistent motion and blocking force profile under cyclic actuation and is robust, remaining functional after more than 100 cycles of actuation. When actuated with a flow rate of 8 mL min^{-1} for 100 cycles, the linear actuator demonstrated a consistent linear motion profile (1.34 ± 0.01 mm) with no drop in linear motion amplitude across the 100 cycles tested (Figure 2F). Testing of linear actuators was limited to 100 cycles due to the testing apparatus and data logging available for this study. The actuators did not fail during testing. In a separate manual actuation testing, the actuator achieved a minimum and maximum length of 4.92 mm and 8.97 mm, indicating a length expansion of 82.24% from the minimum position. For the blocking force testing, the actuator was situated to push against a fixed force sensor lever arm (Figure 2G). Similarly, the measured blocking force profile is consistent across 100 cycles (1.40 ± 0.081 mN) (Figure 2H). During high cycle unloaded testing, linear actuator deflection decreased 45% over a 43 hr period of continuous cyclic actuation (Figure S6, Supporting Information). This represents less than a 0.63×10^{-3}% decrease in deflection amplitude per actuation cycle. Interestingly, after testing, visual inspection of the actuator found that the side had split during testing (Figure S6, Supporting Information, inset). Despite this defect, the actuator was still able to extend and contract.

Testing results of the bending and linear actuator confirm that the FRESH technique can be utilized to build millimeter-scale hydrogel actuators with reliable bending and linear motions. These hydraulic actuators remain functional after hundreds of actuation cycles without structural or operational failure and can even continue to operate over 10s of thousands of cycles. They also exhibit consistent and robust performance over an extended period of operation with a minor decrease in motion amplitude. These actuators with simple actuation geometry lay the foundation for FRESH-printed soft robotic components with complex motion profiles and capabilities.

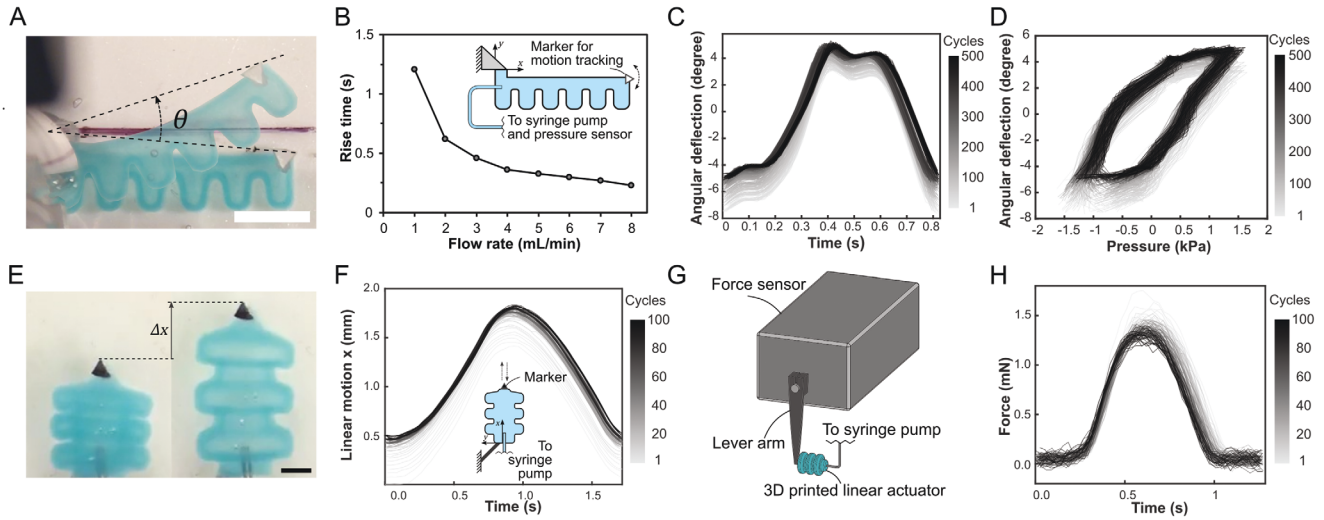

Figure 2. A) Overlaid photos showing the angular deflection of the actuator. Scale bar: 5 mm. B) Actuator rise time as a function of input flow rate. Overlaid actuator angular deflection as a function of C) time and D) input pressure across 500 cycles of loading. E) Photos showing the length change of the actuator. Scale bar: 2 mm. F) Overlaid actuator linear motion as a function of time across 100 cycles of loading. G) Schematic of the force measurement setup of the linear actuator. H) Overlaid actuator force output as a function of time across 100 cycles of loading. See Video S1 (Supporting Information) to see the actuators in motion.

2.2. FRESH-Printing Expands the Design Space for Soft Hydrogel Actuators and Robots

Unlike traditional 3D fabrication techniques, such as casting, embedded printing techniques like FRESH greatly expand geometric design freedom and enable the fabrication of complex 3D structures that are difficult or impossible to achieve with conventional manufacturing techniques. For example, objects with thin walls and enclosed and irregular internal chambers are difficult to fabricate in one piece using mold casting due to casting-related design constraints, such as minimum wall thickness and the need to remove internal mold components post-casting. A common workaround involves casting different actuator parts before assembling them, which requires additional fabrication steps.

We showcased the design flexibility of FRESH for soft robot fabrication by implementing three actuator structures of increasing complexity that are relevant to robotics: (1) a soft gripper, (2) a twisting continuum actuator, and (3) a multi-actuator structure. These structures were fabricated in a single print without requiring multi-part molding or post-printing assembly, as is needed in traditional soft robotics fabrication approaches.

2.2.1. Soft Gripper

A soft hydrogel gripper was created by FRESH printing a structure with two opposing Pneu-Net style actuators (**Figure 3**A). To achieve water-tightness, the gripper was fabricated in the same orientation as the linear actuators (Figure 3B). A single syringe could then be used to drive both fingers of the gripper (Figure 3C). Extracting liquid from the cavity caused the fingers to open (Figure 3D), and pressurizing the structure caused the finger to close (Figure 3E).

2.2.2. Twisting Continuum Actuators

This actuator consists of eight bellow units axially arranged with smooth and twisting joints (Figure 3F). The twisting pattern of the bellows around the central axis, combined with the long aspect ratio, makes this structure very challenging to fabricate by casting, especially when using fragile materials like hydrogels. Upon actuation, these actuators showed a composite actuation motion with a large motion range, which is a combination of extension, bending, and twisting (Figure 3F). Similar to an elephant's trunk, this actuator can provide compliant grasping when manipulating objects of different sizes by wrapping around them (Figure 3G,H). Additionally, it can transform into a soft hook for handling objects too large for its wrapping motion (Figure 3I).

2.2.3. Multi-Actuator Structures

In addition to printing individual actuators with complex morphologies, the FRESH 3D printing approach presented here enables the fabrication of complex, multi-actuator structures that would be otherwise challenging to fabricate. Actuators and their supporting structures can be printed simultaneously in the support bath. To demonstrate this concept, we designed a three-actuator system with inter-actuator truss supports (Figure 3J). Three fluidic channels were inserted into the structural base for each actuator. Each channel can be driven independently by a programmatically controlled syringe pump. Actuating each channel, either separately or in combination, allows the end effector to be positioned in a 3D workspace (Figure 3J). These structures would be challenging to fabricate via casting but can be printed as a single structure with the FRESH printing approach presented here. As a result, this method provides tremendous potential for creating future biodegradable robots that are highly compliant and capable of complex behaviors and motions.

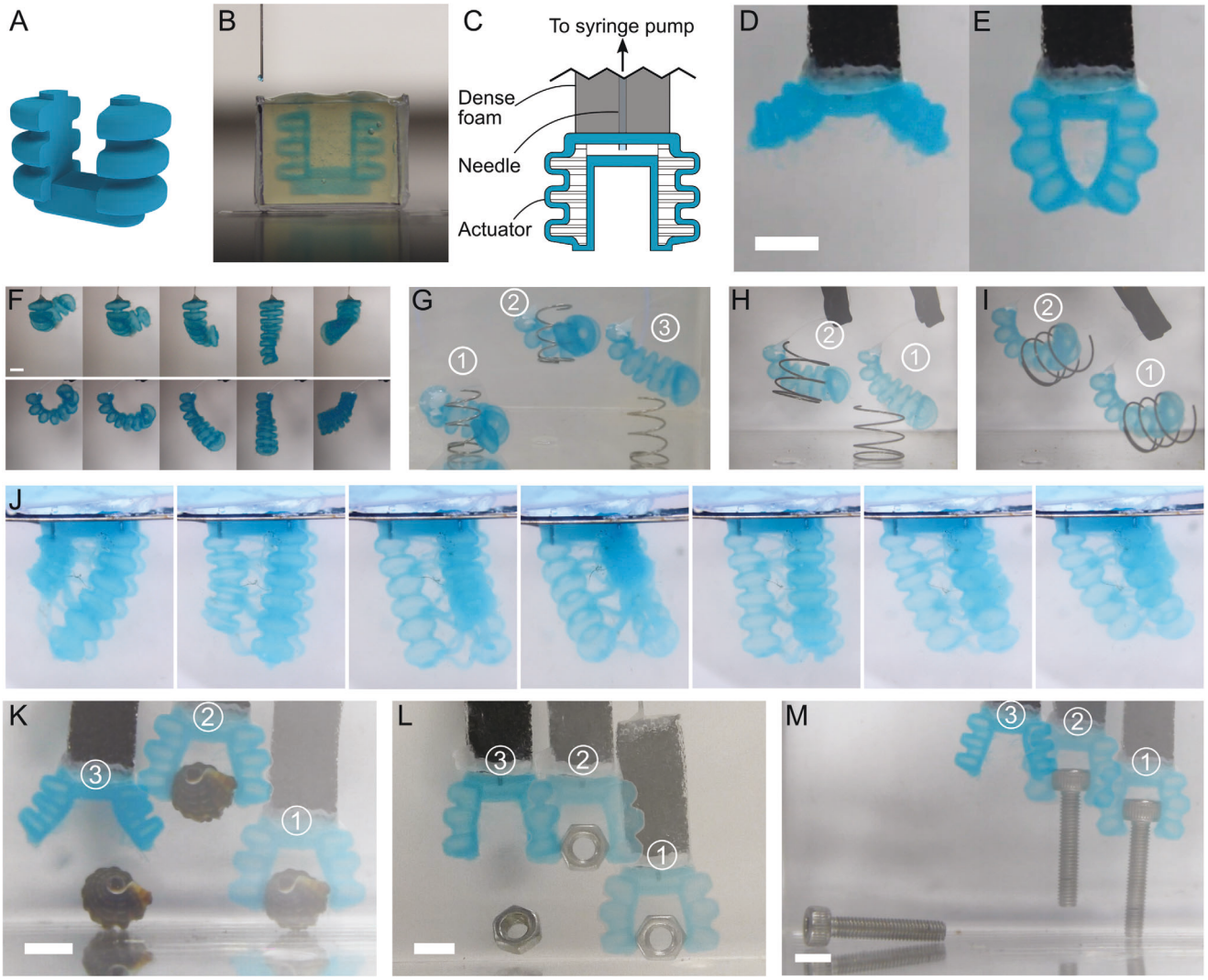

Figure 3. A) CAD model of the soft hydrogel gripper. B) A side view of the FRESH-printed gripper immediately after printing in the support bath. C) Schematic of the gripper and supporting interface with the needle for pressure control. D) FRESH-printed gripper in the open configuration. Scale bar: 5 mm. E) FRESH-printed gripper in the closed configuration. F) Photos of the front (top) and side (bottom) views of actuation in action. From left to right, the actuator begins in a pressurized configuration (panel 1). As the liquid is removed, the actuator untwists (panels 2–3) and returns to the straight configuration (panel 4), after which further fluid extraction causes the actuator to flex backward (panel 5). Scale bar: 5 mm. See Video S4 (Supporting Information) for the actuator in motion. G) The actuator handling a small spring. H,I) The actuator handling a large spring with two motion types. J) FRESH-printed multi-actuator structures can be fabricated with multiple internal cavities and external truss-based support networks that would be otherwise challenging to fabricate. Scale bar: 5 mm. Independent control of each actuator allows the structure to move smoothly and position the end in continuous 3D space with high degrees-of-freedom. K–M) Demonstration of the objection handling capability of FRESH-printed grippers, See Video S2 (Supporting Information). Overlaid photos of the gripper grabbing, moving, and releasing objects, including a (K) sea snail, (L) M3 hex nut, (M) M3 socket head screw. Scale bar: 5 mm.

2.3. Applicability to Small-Scale Objects Manipulation

To highlight the applicability of FRESH-printed hydraulic actuators in soft robotics, we qualitatively assessed the object handling performance of the two-finger soft gripper in an aquatic environment (Figure 3K–M). The FRESH-printed gripper was capable of compliant handling of objects with various surface textures, stiffness, weight, and geometry. One of the potential applications of FRESH-printed actuators is soft robots deployed to operate in marine environments where the brown seaweed from which the alginate ink is derived is native. Therefore, we chose a range of representative and application-relevant objects for gripper testing, including a sea snail shell with a rough surface texture (Figure 3K), an M3 hex nut with a smooth, low-friction surface (Figure 3L), an M3 screw (Figure 3M), and a large section of fragile sea grape (Figure 1D). The gripper was able to grip, lift and move the objects reliably, with a weight lifting capacity of at least 1.02 g, which is 3.4 times the gripper's weight. This capacity is comparable to many previously reported soft grippers, including fluidic elastomer actuators (FEAs)[31,39] and ionic polymer-metal composites-based actuators.[40] These grippers could even function for a limited time in air, and loss of function during

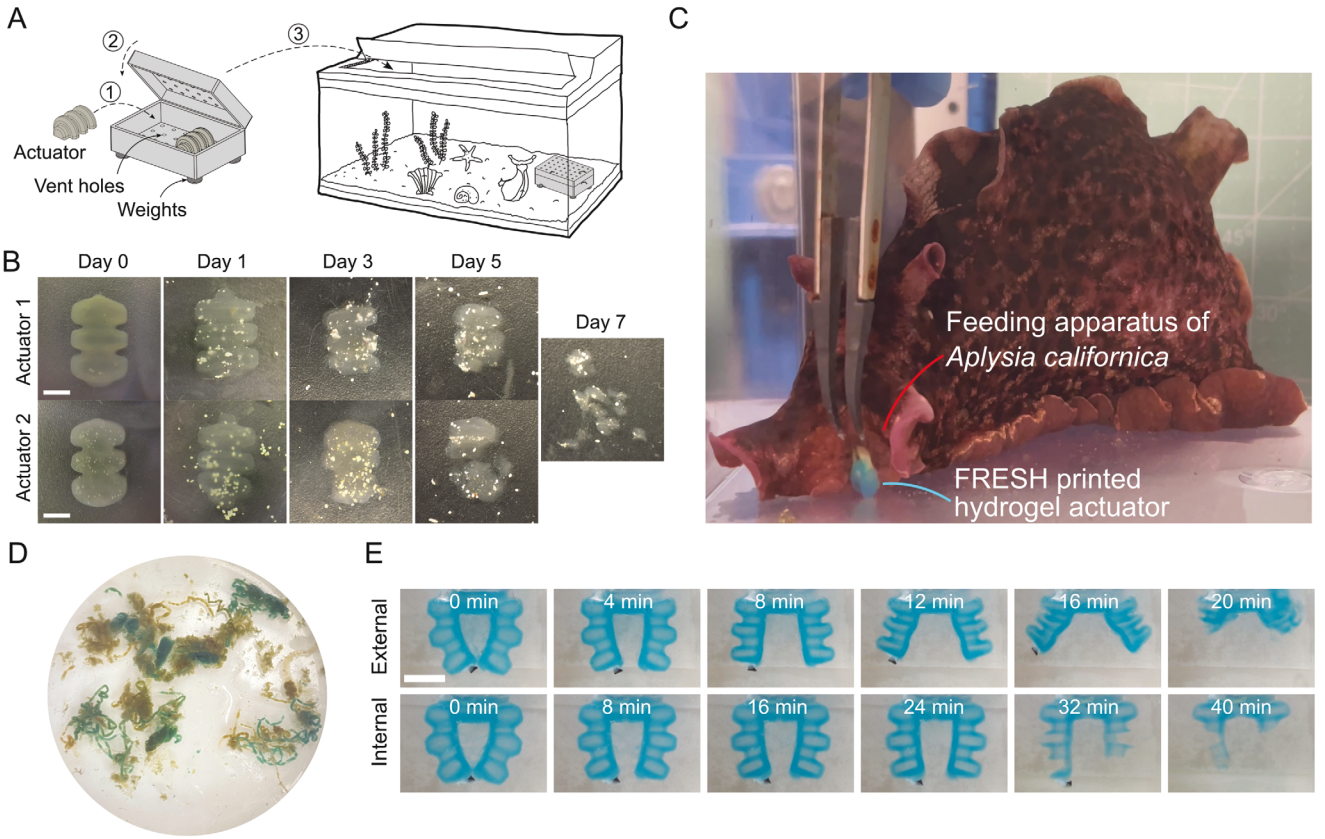

Figure 4. Degradation behavior of FRESH-printed alginate actuators. A) Schematic of the degradation testing setup of FRESH-printed alginate actuators in an aquarium with a variety of living organisms. B) Photos of the degradation results of two alginate actuators across seven days of incubation in the aquarium. Scale bars: 5mm. A timelapse of the results is included in Video S3 (Supporting Information). C) Photo of an *Aplysia californica* feeding on a FRESH-printed alginate actuator. D) Comparison of the digestive detritus of the *Aplysia californica* with normal seaweed (green) and alginate actuators with Alcian Blue dye (blue). E) Rapid degradation of FRESH-printed alginate grippers within 60 min using both external chelation (top) and internal chelation (bottom). Scale bar: 5 mm.

dehydration could be partially regained through rehydration of the structure within a limited window (See Supporting Information). With a millinewton-scale force output and millimeter-scale body size, FRESH-printed hydrogel actuators create opportunities for fluidically actuated soft micromanipulators for delicate object manipulation.

2.4. FRESH-Printed Alginate Actuators are Biodegradable

One of the major challenges for soft robot applications beyond the lab is to address the environmental stresses and hazards associated with traditional, non-biodegradable or even toxic materials. Several strategies have been explored for fabricating soft grippers using environmentally safe materials.[9] For example, soft grippers made of biodegradable polymers (poly(glycerol sebacate))[41] and edible polymers (gelatin-glycerol)[39] have been introduced. However, these actuators are generally made using labor-intensive fabrication techniques that limit their geometric design freedom, such as casting or laser cutting components before gluing them together. Additionally, the degradation of some biodegradable polymers requires elevated temperatures (50–55 °C), which is not readily available in many natural environments.[42]

FRESH-printed actuators used in this study are made of a naturally sourced, sustainable, and biodegradable bioink material, sodium alginate. The fabrication and crosslinking process does not involve the use of harsh chemicals. To assess the biodegradation of FRESH-printed alginate actuators, we first characterized their degradation in an application-relevant environment, a marine reef aquarium with a range of organisms (**Figure 4**A). This study indicates that the alginate actuators experienced degradation in the ambient marine environment (15 °C) within the first week of incubation. No visible residue was found after day 7 (Figure 4B). Furthermore, the degradation speed of alginate actuators can be drastically increased by internal and external chelation. During FRESH printing, newly deposited alginate filaments form highly stable complexes (calcium alginate hydrogels) with the calcium ions in the support bath.[43] Chelators, such as sodium citrate and ethylenediamine tetraacetic acid (EDTA) disodium, can bind to the calcium ions, effectively destabilizing the crosslinked alginate structures. In rapid degradation testing, the alginate actuators could be completely dissolved with the presence of internal and external chelators in less than 60 min (Figure 4E).

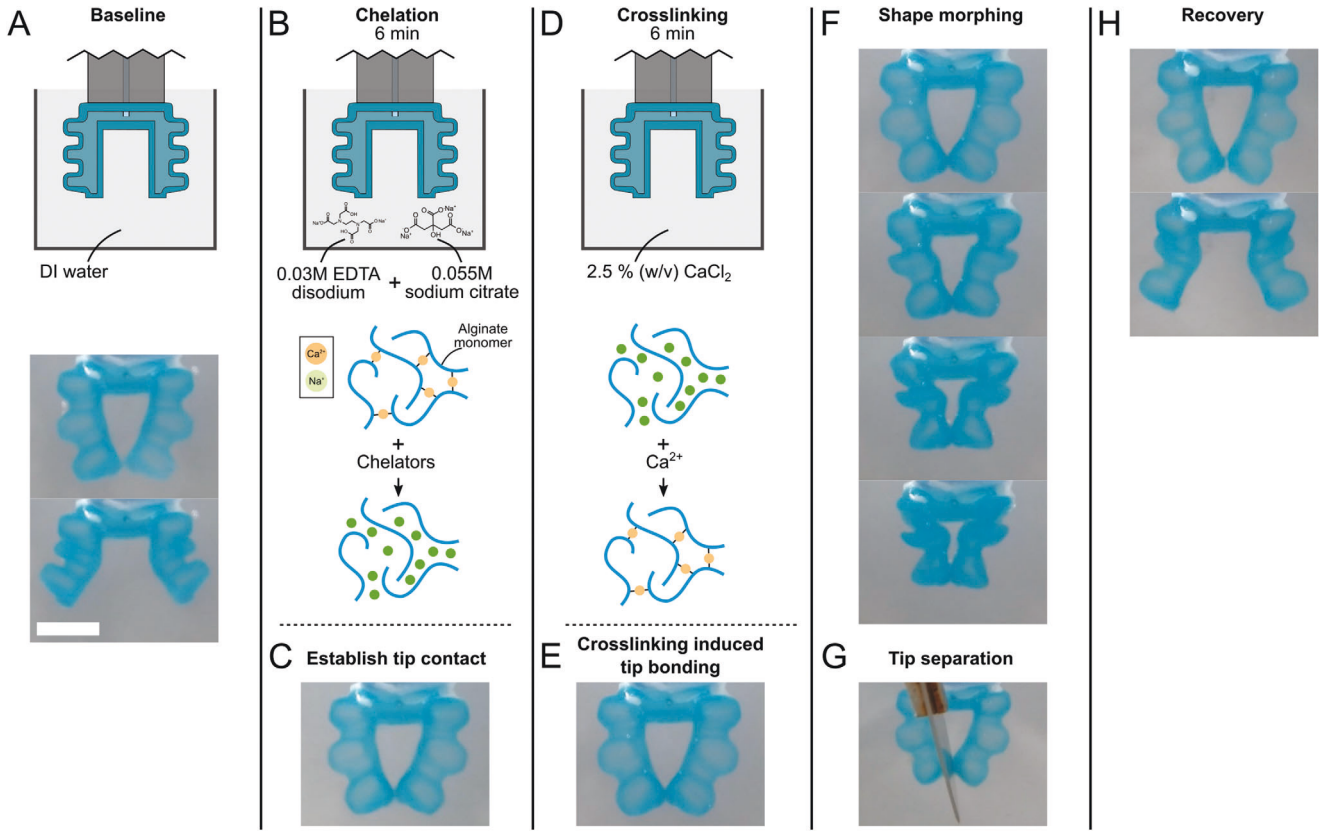

Figure 5. The FRESH-printed alginate gripper demonstrates shape morphing capability based on a reversible chelation-crosslinking mechanism. Before chelation, the gripper exhibited normal closed and open geometry A). Subsequently, the external surface of the gripper was subjected to chelation, freeing up alginate monomers B). The gripper was pressurized to establish tip contact C) before crosslinking D), which induced the bonding of the two tips E). The gripper exhibited a different actuation geometry after the chelation-crosslinking process F). The original actuation geometry was recovered by separating the bonded tips G,H). Scale bar: 5 mm.

2.5. Alginate Actuators are Edible by Marine Life

Another advantage of using plant-derived materials in hydrogel robotic actuators is the possibility that they are safely edible if ingested by native life during deployment. To test whether alginate actuators would be edible for marine life, a feeding study was performed by mixing FRESH-printed actuators into the regular diet of a sea slug. The FRESH-printed alginate actuators in this work were safely edible for the sea slug, which was fed with a mixed diet consisting of normal seaweed and four grippers, and 29 bending actuators (with Alcian Blue dye for visualization) across a period of 29 days (Figure 4C). The size and shape of the digestive detritus from FRESH-printed actuators were similar to those from normal seaweed, indicating that the subject animal could digest a substantial amount of FRESH-printed alginate actuators (Figure 4D).

2.6. FRESH-Printed Alginate Actuators can Undergo Reversible Shape Morphing

The ability to controllably degrade actuators using chelators, as shown in Section 2.4, raises exciting possibilities to create morphing soft robots. In our degradation studies, chelators were found to expedite the degradation of calcium-crosslinked alginate (Figure 4E) by binding to calcium ions from the alginate-calcium complex and exposing alginate monomers. If chelators are applied briefly so as to not fully dissolve the structure, reintroduction of new calcium ions will re-crosslink the monomers.[43,44] We utilized this reversible chelation-crosslinking mechanism to create FRESH-printed alginate grippers that could dynamically change shape from the gripper shown in Figure 3A–E to a round grabber (**Figure 5**). Before chelation, the two fingers of the alginate gripper had normal closing and opening motions upon actuation (Figure 5A). During chelation, free alginate monomers became available on the outer surface of the gripper when chelators in the bath bound to the calcium ions from the calcium-alginate complexes (Figure 5B).[43] The tips of the two fingers were brought into contact by pressurizing the gripper, which formed a temporary connection of alginate monomers (Figure 5C). This pressurization-induced connection method was chosen among other methods, such as using external manipulators to force the two tips into connection, because it eliminates potential damage to the actuator structure during the manipulation step. Furthermore, this temporary alginate monomer bridge can be crosslinked with the introduction of calcium ions and

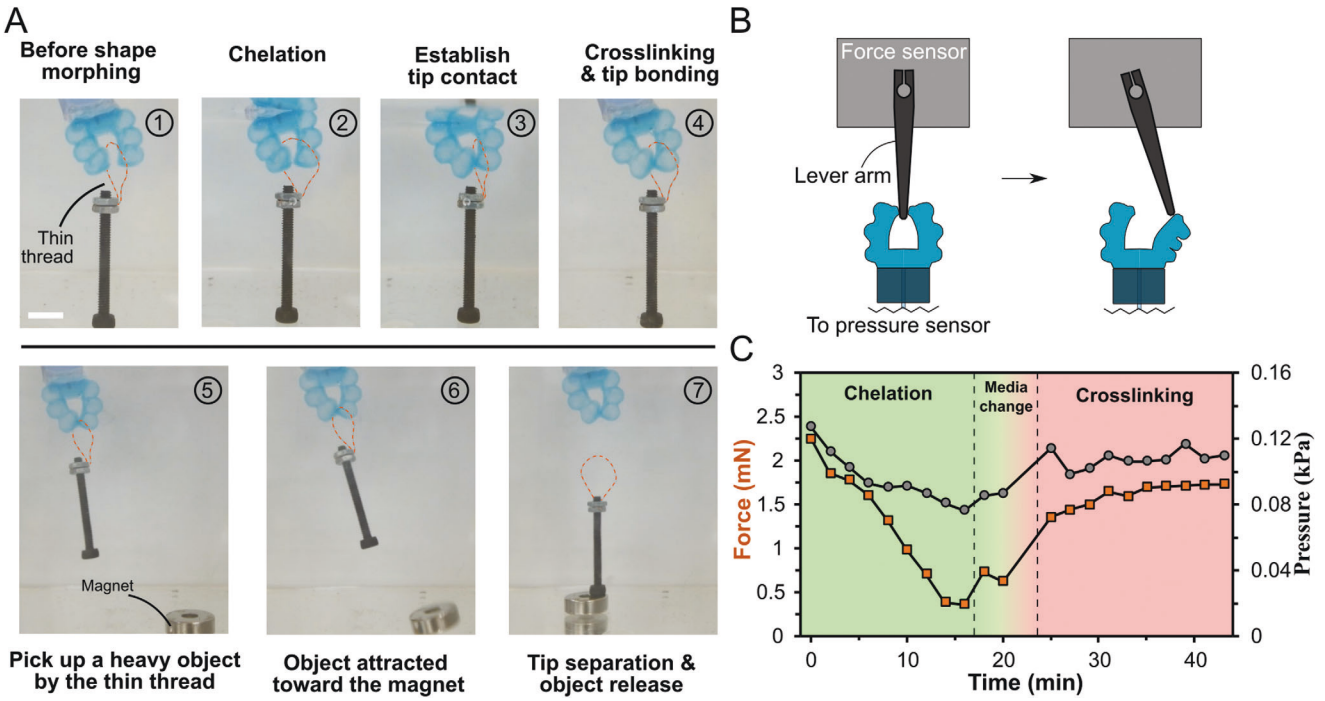

Figure 6. Application and characterization of the shape morphing capability of FRESH-printed alginate gripper. A) Photos of the gripper picking up a heavy object by an attached thin thread after bonding its two fingers using the chelation-crosslinking process, which was later broken and released the object upon arrival at the desired location with increased loading. Red dashed traces of the thread are added for visual enhancement. Scale bar: 5 mm. B) Schematic of the gripper force and pressure measurement setup. C) Gripper finger reaction force (orange squares) and pressure (gray circles) are a function of time and the chelation-crosslinking process.

form a stable calcium-alginate complex that bonds the two fingers together (Figure 5D,E). As a result of this newly introduced structural constraint, when fluid was withdrawn, the gripper contracted instead of opening its two fingers, showing a new actuation geometry (shape morphing) similar to the functionality of a soft robotic grabber[45] (Figure 5F). The original gripper-styled actuation geometry can be recovered by separating the bonded tips (Figure 5G,H).

The chelation-crosslinking induced gripper-grabber shape morphing showcases a unique property of FRESH-printed alginate actuators: the ability to switch between different actuation geometries as needed for a given application. We tested the applicability of post-printing shape morphing through a set of object manipulation tests. One limiting factor of soft grippers for object handling is the object's size. Items significantly smaller than the finger root distance, such as a thin thread (**Figure 6**A), are more likely to slip through the fingers and cause a loss of grip when compared with those with the same weight and larger sizes. Utilizing the gripper-grabber transformation enabled by the chelation-crosslinking mechanism (Figure 5), the loss of grip and subsequent slip-through of small objects can be eliminated by bonding the two fingers and forming a closed loop (Figure 6A). In this case, the reconfigured actuator geometry enables the soft grasper to manipulate the thin thread attached to a small bolt, which was not possible with the original gripper design.

2.7. The Stiffness of FRESH-Printed Alginate Actuators can be Dynamically Tuned during Operation

In addition to adding structural constraints or morphing shape post-printing, the reversible chelation-crosslinking mechanism can also modify the stiffness of alginate actuators by changing the degree of calcium crosslinking as measured by deflection force (Figure 6B). As the chelation proceeded, the gripper's reaction force and internal pressure decreased, indicating a softening of the calcium-alginate hydrogel structure due to a decreasing degree of crosslinking (Figure 6C). In contrast, when additional calcium ions were supplied, both the reaction force and internal pressure increased, indicating a recovery of the rigidity of the alginate structure. It should be noted that, with the chelation-crosslinking protocol tested in this work, this stiffness recovery only occurred during the first chelation-crosslinking cycle. When a second round of chelation was performed on a second sample, the actuator was digested beyond recovery. This is in agreement with our external chelation rapid degradation results, which found that by 20 min of chelation, the actuator ceased to function. This variable degree of crosslinking has the potential for creating soft components with tunable stiffness and force output capacity that satisfy different operational requirements. For example, the gripper could be softened to handle delicate tissues or organisms. However, further process optimization is needed to identify protocols for multi-cycle stiffness changes.

3. Discussion

Made with alginate ink materials sourced from *Lessonia nigrescens* and *Lessonia trabeculata*, two brown seaweed species that are part of the most extensive and productive marine vegetated habitats,[36] the FRESH-printed alginate actuators in this study establish a strategy toward soft robots that are naturally-sourced, biodegradable, and sustainable with minimal negative impact to the environment. Despite the soft hydrogel used for these structures, alginate actuators showed steady mechanical stability over 100s of cycles and maintained functionality over 10s of thousands of actuation cycles. Furthermore, the safely edible nature of their building materials greatly reduces potential risks to animals in case of accidental ingestion. As a result, future FRESH-printed soft robots can potentially be deployed in the field without the need for retrieval, and they are more biodegradable than most existing soft robotic grippers. Such a unique combination of weight lifting capacity and exceptional biodegradability places FRESH-printed actuators in this work into an underexplored domain of soft robotics (Figure 1F).

There are several limitations of the current work that can be explored in future studies. In establishing protocols to ensure FRESH-printed actuators are water-tight, we focused on varying the concentration of the $CaCl_2$ in the support bath and the cartesian orientation of the print relative to the extrusion nozzle. However, research on FRESH printing polymers has found that print quality depends on a number of printing parameters, including extrusion rate, translation speed, and extrusion angle.[46] Properties such as the cross-sectional shape of extruded filaments may play a role in filament-to-filament adhesion. Therefore, future studies should undertake systematic studies of filament fusion within FRESH-printed actuators under a broader range of printing hyperparameters. Additionally, actuators in this study were tested for a few hundred to 10s of thousands of cycles. In contrast, many robotic actuators are rated for tens of thousands to millions of cycles.[47–51] Additional studies are needed to understand how actuator performance changes as actuators fatigue, wear, and degrade, and to identify techniques to minimize such changes based on mission needs. For example, missions with high cycle manipulation of soft, fragile objects will likely have different wear effects on alginate actuators than missions handling abrasive or rigid objects. Therefore, the actuator properties and degradation rates will need to be tuned to mission needs. These properties could be further tuned by chemical crosslinking approaches common in tissue engineering, such as using Genipin or EDC/NHS crosslinking.[52–59]

Furthermore, the actuators presented in this work were all tested in controlled conditions and required tethers for actuation. The need for a tether is a common challenge in both pneumatic and hydraulic robots.[51,60] However, recently, examples of tether-free soft robotic systems have been reported in the literature (e.g., Ref. [60–64]). Techniques from these studies will need to be adapted for interfacing with the very soft alginate hydrogels in this work to support the translation of these biodegradable robots beyond the lab. Translating these actuators beyond the lab may also require advances in adaptable control and microfluidics as the actuators encounter environments with changing salinity, temperatures, and microbiota. Studying actuator performance under real-world variable conditions and understanding the time course of actuator stiffness changes in these environments will be critical for designing appropriate adaptable control systems. Microfluidic systems may be needed to modulate the salinity of the internal working fluid in response to changing external conditions.

Despite these limitations, the FRESH-printed actuators presented here demonstrate new material approaches for soft robotics. As 3D printing technology has advanced, there has been growing interest in 3D printing soft robotic actuators.[21,65–68] The embedded 3D printing fabrication process greatly reduces manufacturing complexity for complex biologically-sourced hydraulic actuators. Although other small-scale hydrogel and elastomer actuators have been reported in the literature, the biocompatibility, biodegradation, and edibility of these actuators have not been broadly reported. Several biodegradable pneumatic actuators have been reported in recent literature, including fully edible bending pneumatic actuators,[69,70] pneumatic grippers,[69] and tube-shaped actuators.[71] However, these actuators have often exhibited low cycle-to-failure rates[69] or required additional coatings for aquatic applications.[71] More recently, biodegradable electrohydraulic actuators have been introduced,[20] which can achieve high cycle numbers in air operation. However, these actuators still rely on conventional fabrication approaches, including casting and component assembly. To our knowledge, no 3D-printed biodegradable hydraulic actuators that are biodegradable, edible, and exhibit shape and stiffness-morphing capabilities have been previously reported in the literature.

4. Conclusion

In this work, we used FRESH 3D printing to manufacture small-scale, biologically-sourced hydraulic actuators with millinewton-scale force output and complex actuation geometry. This printing approach allows complex, robotic structures to be fabricated using a single fabrication process without multi-step casting or post-fabrication assembly of individual actuators. Made with a sustainable biomaterial sourced from brown seaweed, these actuators are biodegradable in marine environments and even safely edible by marine organisms. Additionally, these actuators can dynamically switch between different geometries as needed for a specific application by utilizing a reversible chelation-crosslinking mechanism. This reversible crosslinking also allows the stiffness of individual actuators to be tuned during operation, enabling tunable structural mechanics and force output capacity. Our findings establish a strategy for fabricating biodegradable, sustainable soft robots with post-printing shape morphing capability. These actuators support the future creation of biodegradable robots for deployment in sensitive marine ecosystems.

5. Experimental Section

Materials: Sodium alginate (mannuronic to guluronic acid (M/G) ratio = 1:3, Allevi), Alcian Blue (Alfa Aesar), gelatin Type B (Fisher Chemical), Pluronic F-127 (Sigma–Aldrich), gum arabic (Sigma–Aldrich), hydrochloric acid (HCl) (1N, Fisher Chemical), calcium chloride ($CaCl_2$) (Fisher Chemical), sodium citrate (Innovating Science), ethylenediamine tetraacetic acid (EDTA) disodium (HiMedia), and water-resistant glue (Ultra-Gel Control Super Glue, Loctite) were used as received.

Preparation of Alginate Bioink, Gelatin Support Bath Materials: The alginate bioink used in this study was prepared by solubilizing sodium alginate in heated deionized water (65 °C) to achieve the desired concentration (4% w/v). Optionally, to facilitate visualization during printing and imaging, Alcian Blue was added to the bioink to achieve a concentration of 0.02% (w/v). The gelatin support bath for FRESH printing was made using a complex coacervation process following the previous work with slight modification.[23,29,38] Briefly, 50% (v/v) ethanol was made by mixing ethanol with heated deionized water (70–80 °C). 2.0% (w/v) gelatin Type B, 0.25% (w/v) Pluronic F-127, and 1.0% (w/v) gum arabic were thoroughly mixed in the ethanol solution using magnetic stirring. The gelatin precursor solution was adjusted to 5.550–5.570 pH by adding 1N HCl dropwise using a benchtop pH meter (Apera Instruments). The precursor solution was stirred overnight using an overhead stirrer in a temperature-controlled room (21–24 °C), and the resulting gelatin slurry was washed three times with 0.05% (w/v) $CaCl_2$. To prepare the support bath material for FRESH printing, the slurry was stirred and centrifuged at 2000 g for 5 min prior to printing.

FRESH Printing of Alginate Actuators: All digital models (e.g., Figure S1A, Supporting Information) in this study were created using Solidworks (Dassault Systèmes). Solid models were converted to Geometric codes (G-code) using Slic3r (http://slic3r.org) (20 mm s^{-1} print speed, 80 µm layer height, all perimeter-only pattern in general). Due to the layer-by-layer, extrusion-based printing method, actuator design, and Geometric code (G-code) generation strategy affect the printed actuators' watertightness. Pneu-Net style actuators were sliced so the bellows could be extruded as continuous filaments in each layer (Figure S3B, Supporting Information). In bellow regions where the membrane undergoes considerable strain during actuation, the wall thickness setting in the slicer was kept consistent (500 µm) to reduce stress concentration and ensure consistent crosslinking (Figure S3A, Supporting Information). For the actuator wall opposite the bellows, the wall thickness was set to 700 µm in the slicing program. The wall thickness of the remaining flat surfaces was set to 1 mm. The linear actuator tested in this work has a circularly-symmetric cross-sectional geometry with a wall thickness of 500 µm (Figure S3C, Supporting Information), which allows axial expansion and contraction (Figure 2E). During printing, the hydrogel filament deposition was designed to progress along the axial direction (Figure S3D, Supporting Information). Preliminary trials found that attempts to print the actuators from the transverse direction failed to produce water tightness and should be avoided for this geometry. To eliminate unwanted gaps and cavities that might be created by infill patterns, perimeter-only features were used to create a solid structure throughout the actuator wall during G-code generation (Figure S3B, Supporting Information).

A desktop CoreXY 3D printer (Elf, Creativity Technology) equipped with a Replistruder V4 syringe extruder[72] was used for all 3D printing tasks. Before printing, the bioink was transferred to a 5 mL gastight syringe (Model 1005TLL, Hamilton) with a G30 blunt-tip needle (DN-05-LP-30, Bestean). For short prints (less than 30mm), the G30 needle was attached directly to the bioink syringe through a Luer-lock connection. For tall prints, such as the multi-actuator structures in Section 2.2.3, the needle length was extended by connecting a G23 needle to the syringe and inserting a G30 needle in the open end of the G23 needle via a press fit. Alginate ink was then extruded from the syringe into the $CaCl_2$ doped gelatin support bath at 22 °C (Figure S1B, Supporting Information). After printing, the newly deposited hydrogel structure was kept in the original gelatin slurry at room temperature for 20 min for 10 mm prints (linear actuator, bending actuator, and gripper) and 60 min for 30 mm prints (multi-actuator truss system). The printing chamber was then transferred to a water-tight container with 2.5% (w/v) $CaCl_2$ solution and incubated in a 37 °C water bath for 60 min for slurry liquefaction and part retrieval (Figure S1C, Supporting Information). Subsequently, the printed actuator or structure was transferred to a clean 2.5% (w/v) $CaCl_2$ solution and incubated for 24 h at room temperature (e.g., Figure S1D, Supporting Information). After incubation, the base of the structure was coated with cyanoacrylate and adhered to a silicone block for handling. A dissection pin was used to initially penetrate the actuator membrane to prevent needle clogging, after which a blunt-tipped G25 needle was inserted to create an interface between the actuator and actuation source, such as a syringe pump.

Actuator Deformation, Pressure, and Force Characterization: The angular and linear motion of the bending, and linear actuators were recorded using a digital stereo microscope and quantified using an automatic video analysis software (Tracker 5.1.5, https://physlets.org/tracker). Additional footage of the actuators was recorded using a digital camera (C920, Logitech). Generally, a programmable syringe pump (LEGATO 111, KD Scientific) was used for hydraulic actuation, and an inline pressure sensor (sensor model: MPS2, data reader model: MSR, Elveflow Microfluidics) was used for pressure characterization. A lever arm-based force transducer system (300C-LR, Aurora Scientific) was used for all force measurements. For the linear actuator blocking force measurement, the lever arm was fixed in its position and recorded the force from the linear actuator. Initial tests of the linear and bending actuators were performed under low cycle count conditions (100 and 500 cycles, respectively). Subsequently, to assess the longer-term robustness of these actuators, a subset was subjected to unloaded, high-cycle number testing over 43 h. A bending actuator was driven at 1 Hz and a linear actuator at 0.46 Hz, thereby reaching over 150 000 and 71 000 cycles, respectively.

For the gripper reaction force measurement under variable degrees of crosslinking, the lever arm was initially set to be fixed in its vertical position. The two fingers of the gripper were brought into contact with the lever arm, which was then set to move away from its original position for 2 mm while recording the reaction force from one of the gripper fingers.

Actuator Degradation and Feeding Study: The aquarium used for this study consists of artificial seawater and various marine organisms, including seaweed, sea snails, crabs, and *Aplysia californica* (sea slug). *Aplysia californica* were obtained from Marinus Scientific and South Coast Biomarine and maintained in artificial seawater (Instant Ocean, Aquarium Systems) in aerated aquariums at a temperature of 16 °C for the duration of the study. Two FRESH-printed bending actuators were placed in a plastic container with vent holes, which were placed on the aquarium floor. The container was removed briefly from the aquarium daily for inspection. For the feeding study, the subject animal was fed with four FRESH-printed grippers and 29 bending actuators across a period of 29 days. Animal health and willingness to eat normal seaweed following ingestion of actuators were monitored throughout the study. In the rapid degradation study, the chelator solution consisted of 0.09 M EDTA disodium and 0.165 M sodium citrate. For external chelation, the actuator was submerged in the chelator solution and actuated using 2.5% (w/v) $CaCl_2$ solution. For internal chelation, the actuator was submerged in deionized water and actuated using the chelator solution till failure, after which 3 mL of chelator solution was gradually dispensed through the broken gripper into the bath.

Actuator Shape Morphing: Shape morphing of the gripper presented in this work was achieved through a reversible chelation-crosslinking process.[43,44] After baseline grasper testing, the fluid surrounding the gripper was replaced with a solution of 0.03M EDTA disodium and 0.055M sodium citrate. The gripper was incubated in this chelation solution for 6 min, after which the gripper was manually pressurized to establish tip contact. While maintaining pressure a constant pressure in the gripper, the surrounding fluid was removed and replaced with the 2.5% $CaCl_2$ crosslinking solution. This resulted in bonding between the gripper tips. The morphed gripper was then actuated and exhibited the new grabber morphology. Finally, the tips were manually separated using a scalpel, and the gripper was again actuated to demonstrate recovery of the original gripping behavior.

Actuator Stiffness Morphing: Stiffness morphing was tested using an external chelating agent. The gripper was placed in a 5 mL dish, and the gripper was pressurized until it closed on the lever arm of a length-controlled force-measuring servo motor (300C-LR, Aurora Scientific). The servo-motor was programmed to move 2mm laterally every 2 min, thereby extending one arm of the gripper while measuring the force applied by the gripper arm on the lever arm. Before beginning recording, the media was replaced with a chelating solution of 0.03M EDTA with 0.055M sodium citrate. After 17 min, a 5mL syringe was used to remove the chelation media. The dish was washed twice with 5 mL of DI water over a 3-min window, after which the DI water was removed, and 5 mL of fresh 2.5% $CaCl_2$

solution was introduced to assess the ability to re-crosslink the gripper and increase stiffness. To assess the robustness of the actuator to repeated chelation-crosslinking cycles, this cycle was performed up to two times.

Supporting Information

Supporting Information is available from the Wiley Online Library or from the author.

Acknowledgements

This research was supported in part by grants from the NSF DBI 2015317 as part of the NSF/CIHR/ DFG/FRQ/UKRI-MRC Next Generation Networks for Neuroscience Program, the Presidential Fellowship in the College of Engineering at Carnegie Mellon University, the Collaborative Fellowship from the Department of Mechanical Engineering at Carnegie Mellon University, and funding award no. HQ00342110020 from the National Defense Education Program. Some figures were created with the assistance of Biorender (biorender.com). Manuscript copy-editing for clarity and grammar after initial drafting was assisted by Grammarly and ChatGPT. All edited content was reviewed by the authors. The authors also thank the anonymous reviewers for their feedback during the review process, which has greatly helped to improve this manuscript.

Conflict of Interest

The authors declare no conflict of interest.

Data Availability Statement

The data that support the findings of this study are available from the corresponding author upon reasonable request.

Keywords

3D printing, biodegradability, hydrogel actuators, shape morphing, soft robotics, sustainability

Received: April 2, 2023
Revised: April 28, 2023
Published online:

[1] C. Laschi, B. Mazzolai, M. Cianchetti, *Sci. Rob.* **2016**, *1*, 1.
[2] X. Huang, M. Ford, Z. J. Patterson, M. Zarepoor, C. Pan, C. Majidi, *J. Mater. Chem. B* **2020**, *8*, 4539.
[3] X. Huang, K. Kumar, M. K. Jawed, A. M. Nasab, Z. Ye, W. Shan, C. Majidi, *Sci. Rob.* **2018**, *3*, 2018.
[4] Y. She, C. Li, J. Cleary, H. J. Su, *J. Mech. Robot.* **2015**, *7*, 1.
[5] A. M. Hubbard, R. W. Mailen, M. A. Zikry, M. D. Dickey, J. Genzer, *Soft Matter* **2017**, *13*, 2299.
[6] Y. Dong, J. Wang, X. Guo, S. Yang, M. O. Ozen, P. Chen, X. Liu, W. Du, F. Xiao, U. Demirci, B. F. Liu, *Nat. Commun.* **2019**, *10*, 1.
[7] K. C. Galloway, P. Polygerinos, C. J. Walsh, R. J. Wood, in *2013 16th Int. Conf. on Adv. Robot.*, ICAR **2013**.
[8] C. De Pascali, G. A. Naselli, S. Palagi, R. B. Scharff, B. Mazzolai, *Sci. Rob.* **2022**, *7*, eabn4155.
[9] J. Shintake, V. Cacucciolo, D. Floreano, H. Shea, *Adv. Mater.* **2018**, *30*, 29.
[10] F. Hartmann, M. Baumgartner, M. Kaltenbrunner, *Adv. Mater.* **2021**, *33*, 19.
[11] H. Ceylan, I. C. Yasa, O. Yasa, A. F. Tabak, J. Giltinan, M. Sitti, *ACS Nano* **2019**, *13*, 3353.
[12] T. Billiet, M. Vandenhaute, J. Schelfhout, S. Van Vlierberghe, P. Dubruel, *Biomaterials* **2012**, *33*, 6020.
[13] J. Li, D. J. Mooney, *Nat. Rev. Mater.* **2016**, *1*, 12.
[14] K. Varaprasad, T. Jayaramudu, V. Kanikireddy, C. Toro, E. R. Sadiku, *Carbohydr. Polym.* **2020**, *236*, 116025.
[15] W. Sun, S. Schaffer, K. Dai, L. Yao, A. Feinberg, V. Webster-Wood, *Front. Robot. AI* **2021**, *8*, 1.
[16] M. Nadgorny, Z. Xiao, C. Chen, L. A. Connal, *ACS Appl. Mater. Interfaces* **2016**, *8*, 28946.
[17] C. Cvetkovic, R. Raman, V. Chan, B. J. Williams, M. Tolish, P. Bajaj, M. S. Sakar, H. H. Asada, M. T. A. Saif, R. Bashir, *Proc. Natl. Acad. Sci.* **2014**, *111*, 10125.
[18] H. Son, E. Byun, Y. J. Yoon, J. H. Nam, S. H. Song, C. K. Yoon, *ACS Macro Lett.* **2020**, *9*, 1766.
[19] H. Yuk, S. Lin, C. Ma, M. Takaffoli, N. X. Fang, X. Zhao, *Nat. Commun.* **2017**, *8*.
[20] E. H. Rumley, D. Preninger, A. S. Shomron, P. Rothemund, F. Hartmann, M. Baumgartner, N. Kellaris, A. Stojanovic, Z. Yoder, B. Karrer, C. Keplinger, M. Kaltenbrunner, *Sci. Adv.* **2023**, *9*, eadf5551.
[21] R. L. Truby, M. Wehner, A. K. Grosskopf, D. M. Vogt, S. G. Uzel, R. J. Wood, J. A. Lewis, *Adv. Mater.* **2018**, *30*, 1.
[22] T. J. Hinton, Q. Jallerat, R. N. Palchesko, J. H. Park, M. S. Grodzicki, H.-J. Shue, M. H. Ramadan, A. R. Hudson, A. W. Feinberg, *Sci. Adv.* **2015**, *1*, 1.
[23] A. Lee, A. R. Hudson, D. J. Shiwarski, J. W. Tashman, T. J. Hinton, S. Yerneni, J. M. Bliley, P. G. Campbell, A. W. Feinberg, *Science* **2019**, *365*, 482.
[24] J. T. Muth, D. M. Vogt, R. L. Truby, Y. Mengüç, D. B. Kolesky, R. J. Wood, J. A. Lewis, *Adv. Mater.* **2014**, *26*, 6307.
[25] R. D. Weeks, R. L. Truby, S. G. Uzel, J. A. Lewis, *Adv. Mater.* **2023**, *35*, 2206958.
[26] R. L. Truby, J. A. Lewis, *Nature* **2016**, *540*, 371.
[27] J. Zhao, N. He, *J. Mater. Chem. B* **2020**, *8*, 10474.
[28] L.-Y. Zhou, J. Fu, Y. He, *Adv. Funct. Mater.* **2020**, *30*, 2000187.
[29] E. Mirdamadi, J. W. Tashman, D. J. Shiwarski, R. N. Palchesko, A. W. Feinberg, *ACS Biomater. Sci. Eng.* **2020**, *6*, 6453.
[30] Y. Hu, T. Lan, G. Wu, Z. Zhu, W. Chen, *Nanoscale* **2014**, *6*, 12703.
[31] R. Deimel, O. Brock, *Int. J. Rob. Res.* **2016**, *35*, 161.
[32] T. T. Hoang, P. T. Phan, M. T. Thai, N. H. Lovell, T. N. Do, *Adv. Mater. Technol.* **2020**, *5*, 1.
[33] C. Tawk, A. Gillett, G. M. Spinks, G. Alici, *IEEE Trans. Robot.* **2019**, *35*, 1268.
[34] G. K. Lau, K. R. Heng, A. S. Ahmed, M. Shrestha, *Appl. Phys. Lett.* **2017**, *110*, 18.
[35] U. Deole, R. Lumia, M. Shahinpoor, M. Bermudez, *J. Micro-Nano Mechatron.* **2008**, *4*, 95.
[36] K. Kabumoto, K. Toyama, T. Hoshino, K. Morishima, in *2011 IEEE 24th Int. Conf. on Micro Electro Mech. Syst.* **2011**, pp. 1277.
[37] B. Mosadegh, P. Polygerinos, C. Keplinger, S. Wennstedt, R. F. Shepherd, U. Gupta, J. Shim, K. Bertoldi, C. J. Walsh, G. M. Whitesides, *Adv. Funct. Mater.* **2014**, *24*, 2163.
[38] W. Sun, J. W. Tashman, D. J. Shiwarski, A. W. Feinberg, V. A. Webster-Wood, *ACS Biomater. Sci. Eng.* **2021**, *8*, 303.
[39] J. Shintake, H. Sonar, E. Piskarev, J. Paik, D. Floreano, *2017 IEEE Int. Conf. on Intell. Robots and Syst.*, **2017**, pp. 6221 – 6226.
[40] E. Hamburg, V. Vunder, U. Johanson, F. Kaasik, A. Aabloo, *Electroact. Polym Actuators Devices (EAPAD) 2016* **2016**, *9798*, 97981Q.
[41] S. Walker, J. Rueben, T. V. Volkenburg, S. Hemleben, C. Grimm, J. Simonsen, Y. Mengüç, *Int. J. Intell. Robot. Appl.* **2017**, *1*, 124.

[42] E. Rudnik, D. Briassoulis, *J. Polym. Environ.* **2011**, *19*, 18.
[43] J. T. Delaney, A. R. Liberski, J. Perelaer, U. S. Schubert, *Soft Matter* **2010**, *6*, 866.
[44] F. Abasalizadeh, S. V. Moghaddam, E. Alizadeh, E. Akbari, E. Kashani, S. M. B. Fazljou, M. Torbati, A. Akbarzadeh, *J. Biol. Eng.* **2020**, *14*, 1.
[45] M. Schaffner, J. A. Faber, L. Pianegonda, P. A. Rühs, F. Coulter, A. R. Studart, *Nat. Commun.* **2018**, *9*, 1.
[46] T. J. Hinton, A. Hudson, K. Pusch, A. Lee, A. W. Feinberg, *ACS Biomater. Sci. Eng.* **2016**, *2*, 1781.
[47] Y. Guo, L. Liu, Y. Liu, J. Leng, *Adv. Intell. Syst.* **2021**, *3*, 2000282.
[48] Z. Ma, D. Sameoto, *Micromachines* **2022**, *13*, 1881.
[49] M. Ilami, H. Bagheri, R. Ahmed, E. O. Skowronek, H. Marvi, *Adv. Mater.* **2021**, *33*, 2003139.
[50] J. Zhang, J. Sheng, C. T. O'Neill, C. J. Walsh, R. J. Wood, J.-H. Ryu, J. P. Desai, M. C. Yip, *IEEE Trans. Robot.* **2019**, *35*, 761.
[51] N. El-Atab, R. B. Mishra, F. Al-Modaf, L. Joharji, A. A. Alsharif, H. Alamoudi, M. Diaz, N. Qaiser, M. M. Hussain, *Adv. Intell. Syst.* **2020**, *2*, 2000128.
[52] N. A. Peppas, A. G. Mikos, in *Hydrogels in Medicine and Pharmacy*, CRC Press, Boca Raton, FL, USA **2019**, pp. 1–26.
[53] S. K. Gulrez, S. Al-Assaf, G. O. Phillips, in *Progress in Molecular and Environmental Bioengineering-From Analysis and Modeling to Technology Applications*, Intech Europe, Croatia **2011**, pp. 117–150.
[54] J. Maitra, V. K. Shukla, *Am. J. Polym. Sci* **2014**, *4*, 25.
[55] Y. Zhao, Z. Sun, *Int. J. Food Prop.* **2017**, *20*, S2822.
[56] S.-C. Chen, Y.-C. Wu, F.-L. Mi, Y.-H. Lin, L.-C. Yu, H.-W. Sung, *J. Controlled Release* **2004**, *96*, 285.
[57] L. Gao, H. Gan, Z. Meng, R. Gu, Z. Wu, L. Zhang, X. Zhu, W. Sun, J. Li, Y. Zheng, G. Dou, *Colloids Surf., B* **2014**, *117*, 398.
[58] J. Skopinska-Wisniewska, M. Tuszynska, E. Olewnik-Kruszkowska, *Materials* **2021**, *14*, 2.
[59] M. Yan, X. An, Z. Jiang, S. Duan, A. Wang, X. Zhao, Y. Li, *Polym. Degrad. Stab.* **2022**, *200*, 109929.
[60] S. I. Rich, R. J. Wood, C. Majidi, *Nat. Electron.* **2018**, *1*, 102.
[61] A. Kotikian, C. McMahan, E. C. Davidson, J. M. Muhammad, R. D. Weeks, C. Daraio, J. A. Lewis, *Sci. Rob.* **2019**, *4*, eaax7044.
[62] D. Drotman, S. Jadhav, D. Sharp, C. Chan, M. T. Tolley, *Sci. Rob.* **2021**, *6*, eaay2627.
[63] M. T. Tolley, R. F. Shepherd, B. Mosadegh, K. C. Galloway, M. Wehner, M. Karpelson, R. J. Wood, G. M. Whitesides, *A Resilient, Untethered Soft Robot.Soft Robotics.Sep* **2014**, *1*, 213.
[64] Z. J. Patterson, D. K. Patel, S. Bergbreiter, L. Yao, C. Majidi, *Soft Robotics* **2023**, *10*, 292.
[65] E. Thompson-Bean, R. Das, A. McDaid, *Bioinspir. Biomim.* **2016**, *11*, 066005.
[66] J. Z. Gul, M. Sajid, M. M. Rehman, G. U. Siddiqui, I. Shah, K.-H. Kim, J.-W. Lee, K. H. Choi, *Sci. Technol. Adv. Mater.* **2018**, *19*, 243.
[67] T. Wallin, J. Pikul, R. F. Shepherd, *Nat. Rev. Mater.* **2018**, *3*, 84.
[68] E. Sachyani Keneth, A. Kamyshny, M. Totaro, L. Beccai, S. Magdassi, *Adv. Mater.* **2021**, *33*, 2003387.
[69] J. Shintake, H. Sonar, E. Piskarev, J. Paik, D. Floreano, in *2017 IEEE/RSJ Int. Conf. on Intell. Robots and Syst. (IROS)*, IEEE, **2017**, pp. 6221–6226.
[70] A. Heiden, D. Preninger, L. Lehner, M. Baumgartner, M. Drack, E. Woritzka, D. Schiller, R. Gerstmayr, F. Hartmann, M. Kaltenbrunner, *Sci. Robot.* **2022**, *7*, eabk2119
[71] M. Baumgartner, F. Hartmann, M. Drack, D. Preninger, D. Wirthl, R. Gerstmayr, L. Lehner, G. Mao, R. Pruckner, S. Demchyshyn, L. Reiter, M. Strobel, T. Stockinger, D. Schiller, S. Kimeswenger, F. Greibich, G. Buchberger, E. Bradt, S. Hild, S. Bauer, M. Kaltenbrunner, *Nat. Mater.* **2020**, *19*, 1102.
[72] J. W. Tashman, D. J. Shiwarski, A. W. Feinberg, *HardwareX* **2021**, *9*, e00170.